
**FINITE-DIFFERENCE TIME-DOMAIN
CALCULATIONS BASED ON RECURSIVE
CONVOLUTION APPROACH FOR PROPAGATION
OF ELECTROMAGNETIC WAVES IN NONLINEAR
DISPERSIVE MEDIA**

S. Joe Yakura and Jeff MacGillivray

30 October 1997

Final Report

19980210 068

APPROVED FOR PUBLIC RELEASE; DISTRIBUTION IS UNLIMITED.



**AIR FORCE RESEARCH LABORATORY
Directed Energy Directorate
3550 Aberdeen Ave SE
AIR FORCE MATERIEL COMMAND
KIRTLAND AIR FORCE BASE, NM 87117-5776**

PL-TR-97-1170

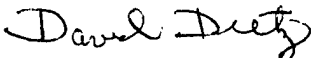
Using Government drawings, specifications, or other data included in this document for any purpose other than Government procurement does not in any way obligate the U.S. Government. The fact that the Government formulated or supplied the drawings, specifications, or other data, does not license the holder or any other person or corporation; or convey any rights or permission to manufacture, use, or sell any patented invention that may relate to them.

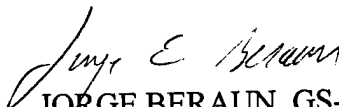
This report has been reviewed by the Public Affairs Office and is releasable to the National Technical Information Service (NTIS). At NTIS, it will be available to the general public, including foreign nationals.

If you change your address, wish to be removed from this mailing list, or your organization no longer employs the addressee, please notify AFRL/DEPE, 3550 Aberdeen Ave SE, Kirtland AFB, NM 87117-5776.


Do not return copies of this report unless contractual obligations or notice on a specific document requires its return.

This report has been approved for publication.


DAVID DIETZ, GS-14
Project Manager


JORGE BERAUN, GS-14
Chief, DE Effects Research Branch

FOR THE COMMANDER


R. EARL GOOD, SES
Director, Directed Energy Directorate

REPORT DOCUMENTATION PAGE

Form Approved
OMB No. 074-0188

Public reporting burden for this collection of information is estimated to average 1 hour per response, including the time for reviewing instructions, searching existing data sources, gathering and maintaining the data needed, and completing and reviewing this collection of information. Send comments regarding this burden estimate or any other aspect of this collection of information, including suggestions for reducing this burden to Washington Headquarters Services, Directorate for Information Operations and Reports, 1215 Jefferson Davis Highway, Suite 1204, Arlington, VA 22202-4302, and to the Office of Management and Budget, Paperwork Reduction Project (0704-0188), Washington, DC 20503

1. AGENCY USE ONLY (Leave blank)	2. REPORT DATE Oct. 30, 1997	3. REPORT TYPE AND DATES COVERED Final, May 97 - Oct 97	
4. TITLE AND SUBTITLE Finite-Difference Time-Domain Calculations Based on Recursive Convolution Approach for Propagation of Electromagnetic Waves in Nonlinear Dispersive Media			5. FUNDING NUMBERS PE: 62601F PR: 5797 TA: AL WU: 05
6. AUTHOR(S) S. Joe Yakura and Jeff MacGillivray			
7. PERFORMING ORGANIZATION NAME(S) AND ADDRESS(ES) Air Force Research Laboratory /Directed Energy Directorate 3550 Aberdeen Avenue SE Kirtland AFB, NM 87117-5776			8. PERFORMING ORGANIZATION REPORT NUMBER PL-TR-97-1170
9. SPONSORING / MONITORING AGENCY NAME(S) AND ADDRESS(ES)			10. SPONSORING / MONITORING AGENCY REPORT NUMBER
11. SUPPLEMENTARY NOTES			
12a. DISTRIBUTION / AVAILABILITY STATEMENT Approved for public release; distribution is unlimited.			12b. DISTRIBUTION CODE
13. ABSTRACT (Maximum 200 Words) The piecewise linear recursive convolution (PLRC) approach has been shown to provide much improved accuracy over the usual discrete recursive convolution approach while retaining the efficient use of computer memory storage and fast computational speed for finite-difference time-domain (FDTD) electromagnetic propagation calculations for linear dispersive materials. In this paper, an idea behind the implementation of the PLRC approach is extended to handle nonlinear dispersive media, specifically for the convolution integral that depends on the product of the electric field squared and the third-order electric susceptibility function. Compared to linear dispersive material, where one has a simple linear relationship for the next time step electric field as a function of the previous time step electric field, the nonlinear dispersive material case has a cubic equation for the next time step electric field as a function of the previous time step electric field. Consequently, the cubic equation must be solved at successive times to advance the electric field in the next time step.			
14. SUBJECT TERMS Electromagnetics, Nonlinear-Optics, Numerical Analysis			15. NUMBER OF PAGES 30
			16. PRICE CODE
17. SECURITY CLASSIFICATION OF REPORT Unclassified	18. SECURITY CLASSIFICATION OF THIS PAGE Unclassified	19. SECURITY CLASSIFICATION OF ABSTRACT Unclassified	20. LIMITATION OF ABSTRACT Unlimited

TABLE OF CONTENTS

	<u>Page</u>
<i>List of Figures</i>	iv
<i>Abstract</i>	1
<i>I. Introduction</i>	1
<i>II. Governing Equations and General Formulation</i>	3
<i>III. Numerical Analysis - A Case Study for Nonlinear Soliton Formation</i>	7
<i>IV. Conclusions</i>	10
<i>References</i>	17
<i>Appendix</i>	20

LIST OF FIGURES

<u>Figure</u>	<u>Title</u>	<u>Page</u>
1	Illustration of Piecewise Linear Approximation for the Electric Field as a Function of Discrete Time Steps	11
2	Perspective plots of the electric field intensity versus spatial location from linear dispersive calculations taken at five successive times of T_1, T_2, T_3, T_4 and T_5 in order to show the space-time evolution of the optical pulse with the initial pulse width of 3.5 fs. [$T_1 = 10,000\Delta t (=0.083 \text{ ps})$; $T_2 = 40,000\Delta t (=0.333 \text{ ps})$; $T_3 = 70,000\Delta t (=0.583 \text{ ps})$; $T_4 = 100,000\Delta t (=0.833 \text{ ps})$; $T_5 = 130,000\Delta t (=1.083 \text{ ps})$ with $\Delta t = 8.33 \times 10^{-18}$ second]	12
3	Perspective plots of the electric field intensity versus spatial location from nonlinear dispersive calculations taken at five successive times of T_1, T_2, T_3, T_4 and T_5 in order to show the space-time evolution of the optical pulse with the initial pulse width of 3.5 fs. [$T_1 = 10,000\Delta t (=0.083 \text{ ps})$; $T_2 = 40,000\Delta t (=0.333 \text{ ps})$; $T_3 = 70,000\Delta t (=0.583 \text{ ps})$; $T_4 = 100,000\Delta t (=0.833 \text{ ps})$; $T_5 = 130,000\Delta t (=1.083 \text{ ps})$ with $\Delta t = 8.33 \times 10^{-18}$ second]	13
4	Perspective plots of the electric field intensity versus spatial location from linear dispersive calculations taken at five successive times of T_1, T_2, T_3, T_4 and T_5 in order to show the space-time evolution of the optical pulse with the initial pulse width of 7.0 fs. [$T_1 = 10,000\Delta t (=0.083 \text{ ps})$; $T_2 = 40,000\Delta t (=0.333 \text{ ps})$; $T_3 = 70,000\Delta t (=0.583 \text{ ps})$; $T_4 = 100,000\Delta t (=0.833 \text{ ps})$; $T_5 = 130,000\Delta t (=1.083 \text{ ps})$ with $\Delta t = 8.33 \times 10^{-18}$ second]	14
5	Perspective plots of the electric field intensity versus spatial location from nonlinear dispersive calculations taken at five successive times of T_1, T_2, T_3, T_4 and T_5 in order to show the space-time evolution of the optical pulse with the initial width of 7.0 fs. [$T_1 = 10,000\Delta t (=0.083 \text{ ps})$; $T_2 = 40,000\Delta t (=0.333 \text{ ps})$; $T_3 = 70,000\Delta t (=0.583 \text{ ps})$; $T_4 = 100,000\Delta t (=0.833 \text{ ps})$; $T_5 = 130,000\Delta t (=1.083 \text{ ps})$ with $\Delta t = 8.33 \times 10^{-18}$ second]	15

- 6 Comparison of solitary wave packets obtained in the nonlinear 16
dispersive medium from launching two different width pulses
in free space. The solid line is from the optical pulse width
of 7.0 fs and the dashed line is from the optical pulse width
of 3.5 fs. These are taken at the time step of 100,000.

Finite-Difference Time-Domain Calculations Based on Recursive Convolution Approach For Propagation of Electromagnetic Waves in Nonlinear Dispersive Media

S. J. Yakura and J. T. McGillivray
Air Force Research Laboratory, AFRL/DEPE
Kirtland AFB, NM 87117-5776
(30 October 1997)

Abstract

The piecewise linear recursive convolution (PLRC) approach has been shown to provide much improved accuracy over the usual discrete recursive convolution approach while retaining the efficient use of computer memory storage and fast computational speed for finite-difference time-domain electromagnetic propagation calculations for linear dispersive materials. In this paper, an idea behind the implementation of the PLRC approach is extended to handle nonlinear dispersive media, specifically for the convolution integral that depends on the product of the electric field squared and the third-order electric susceptibility function. Compared to linear dispersive material, where one has a simple linear relationship for the next time step electric field as a function of the previous time step electric field, the nonlinear dispersive material case has a cubic equation for the next time step electric field as a function of the previous time step electric field. Consequently, the cubic equation must be solved at successive times to advance the electric field in the next time step.

I. INTRODUCTION

There has been considerable interest in understanding the transient behavior of an ultrafast laser pulse that interacts with nonlinear dispersive materials. In the last several years many experimentalists have made use of the newly developed Kerr-lense mode-locked Titanium-Sapphire lasers to perform well-controlled experiments so that they can obtain accurate transient behavior measurements of ultrafast laser pulses in simple molecular liquids and solids that are known to exhibit nonlinear optical effects [1]. To better understand the details of the nonlinear processes that are observed in experiments, numerical simulation has been used extensively in reproducing the observed nonlinear effects. Until recently most computer simulation has been performed by solving approximated Maxwell's equations, known as the generalized nonlinear Schrodinger (GNLS) equation [2], for the envelope of the propagating oscillating wave packet that provides information on the time evolution of the overall shape of the optical pulse. Since computer simulation based on the GNLS equations could not simply provide any information about oscillating waves contained within the envelope of the optical pulse, there is a renewed interest in obtaining the greater details of propagating optical pulse

phenomena by carrying out computer simulation of Maxwell's equations directly.

In the last few years, computer technology has advanced to the point where arithmetic processing chips can operate up to hundreds of hertz and dynamic random memory chips can hold in excess of multi-giga bytes of memory. Using the present day computers, we can consider solving Maxwell's equations directly without having to rely on approximated Maxwell's equations. Of recently investigated numerical techniques which showed the promising future is the well-known finite-difference time-domain (FDTD) method [3] that is based on a simple differencing scheme in both time and space to calculate transient behavior of electromagnetic (EM) field quantities. Because of the usefulness of the FDTD method for many optical applications, recent researchers have focused their attention into numerical handling of linear and nonlinear polarization terms which appear in one of Maxwell's equations as convolution integrals so that they can simulate linear and nonlinear dispersive effects more effectively [4-9].

Depending on the form of the integrand appearing in the convolution integral, the dispersive effect can be classified as linear or nonlinear. For linear dispersive materials, the relationship between displacement field vector \underline{D} and electric field vector \underline{E} is usually expressed in the following form

$$\underline{D}(t) = \epsilon_o \epsilon_\infty \underline{E}(t) + \epsilon_o \sum_p \int_0^t \underline{E}(\tau) X_p^{(1)}(t-\tau) d\tau \quad (1.1)$$

where ϵ_o is the electric permittivity of free space, ϵ_∞ is the permittivity at infinite frequency, and $X_p^{(1)}(t-\tau)$ is the p th term first-order electric susceptibility function that depends on time difference $(t-\tau)$.

For materials that show both the linear and nonlinear polarization properties, specifically through the first-order (linear) and third-order (nonlinear) electric susceptibility functions, $X_p^{(1)}(t-\tau)$ and $X_p^{(3)}(t,\tau,t_1,t_2)$, respectively, the relationship between D and E can be expressed in the following form

$$\begin{aligned} \underline{D}(t) = & \epsilon_o \epsilon_\infty \underline{E}(t) + \epsilon_o \sum_p \int_0^t \underline{E}(\tau) X_p^{(1)}(t-\tau) d\tau \\ & + \epsilon_o \sum_p \int_0^t \int_0^t \int_0^t \underline{E}(t-\tau) \underline{E}(t-t_1) \underline{E}(t-t_2) X_p^{(3)}(t,\tau,t_1,t_2) d\tau dt_1 dt_2 \end{aligned} \quad (1.2)$$

where $X_p^{(3)}(t,\tau,t_1,t_2)$ is the p th term four-time dependent third-order susceptibility function which contributes to the nonlinear behavior of the material.

Reducing $X_p^{(3)}(t,\tau,t_1,t_2)$ to the one-time dependent susceptibility function, $\chi_p^{(3)}(t_1-t_2)$, by use of the following Born-Oppenheimer approximation [10],

$$X_p^{(3)}(t,\tau,t_1,t_2) = \delta(t-t_1) \delta(\tau-t_2) [\chi_p^{(3)}(t_1-t_2) + \alpha_{0p}^{(3)} \delta(t-t_2)] \quad (1.3)$$

where $\alpha_{0p}^{(3)}$ is a constant and $\delta(t)$ is the Dirac delta function, we can reduce Eq.(1.2) to a more amenable expression that consists of the sum of linear and nonlinear convolution integrals of the form

$$\begin{aligned} \underline{D}(t) = & \epsilon_o \epsilon_\infty \underline{E}(t) + \epsilon_o \sum_\rho \int_0^t \underline{E}(\tau) \chi_\rho^{(1)}(t-\tau) d\tau \\ & + \epsilon_o \underline{E}(t) \sum_\rho \left(\int_0^t [\underline{E}(\tau)]^2 [\chi_\rho^{(3)}(t-\tau) + \alpha_{0\rho}^{(3)} \delta(t-\tau)] d\tau \right) \end{aligned} \quad (1.4)$$

Based on the above expression, this paper provides the general formulation of the FDTD method, which we call the piecewise continuous recursive convolution (PCRC) method, to evaluate the linear and nonlinear single convolution integrals. We investigate specifically the case in which both the first-order and third-order electric susceptibility functions are expressed in the following exponential forms

$$\chi_\rho^{(1)}(t) = \text{Real} \{ \alpha_\rho^l \exp[-\gamma_\rho^l t] \} U(t) \quad (1.5)$$

$$\chi_\rho^{(3)}(t) = \text{Real} \{ \alpha_\rho^{nl} \exp[-\gamma_\rho^{nl} t] \} U(t) \quad (1.6)$$

where $U(t)$ is the unit step function and α_ρ^l , α_ρ^{nl} , γ_ρ^l and γ_ρ^{nl} are complex constants.

By making proper choices of complex constants and carrying out the Fourier Transform, we can readily obtain the familiar Debye and Lorentz forms of the complex permittivity from the above exponential forms.

II. GOVERNING EQUATIONS AND GENERAL FORMULATION

Starting with Maxwell's equations, we can express the following differential equations for spatial and time dependent EM field quantities inside the dispersive material.

$$\underline{\nabla} \times \underline{H}(t) = \frac{\partial \underline{D}(t)}{\partial t} + \sigma \underline{E}(t) \quad (2.1)$$

$$\underline{\nabla} \times \underline{E}(t) = -\frac{\partial(\mu \underline{H}(t))}{\partial t} \quad (2.2)$$

$$\begin{aligned} \underline{D}(t) = & \epsilon_o \epsilon_\infty \underline{E}(t) + \epsilon_o \sum_\rho \underline{P}_\rho^l(t) \\ & + \epsilon_o \underline{E}(t) \sum_\rho \left(P_\rho^{nl}(t) + \alpha_{0\rho}^{(3)} \int_0^t [\underline{E}(\tau)]^2 \delta(t-\tau) d\tau \right) \end{aligned} \quad (2.3)$$

$$\underline{P}_\rho^l(t) \equiv \int_0^t \underline{E}(\tau) \chi_\rho^{(1)}(t-\tau) d\tau \quad (2.4)$$

$$P_\rho^{nl}(t) \equiv \int_0^t [\underline{E}(\tau)]^2 \chi_\rho^{(3)}(t-\tau) d\tau \quad (2.5)$$

where H is the magnetic field vector, D is the displacement field vector, E is the electric field vector, σ is the electrical conductivity, μ is the magnetic permeability, ϵ_0 is the free space electric permittivity, ϵ_∞ is the permittivity at infinite frequency, $X_\rho^{(1)}$ and $\chi_\rho^{(3)}$ are the ρ th term first-order and third-order electrical susceptibilities, and P_ρ^l and P_ρ^{nl} are related to the ρ th term linear and nonlinear polarization field vectors.

Using FDTD the above equations can be solved numerically at each time step, provided $P_\rho^l(t)$ and $P_\rho^{nl}(t)$ are handled properly. Thus, the whole problem rests upon proper numerical evaluation of $P_\rho^l(t)$ and $P_\rho^{nl}(t)$ at each time step. For that reason, the rest of this section is devoted to the discussion of the numerical formulation used to solve $P_\rho^l(t)$ and $P_\rho^{nl}(t)$.

In order to achieve better accuracy in evaluating the convolution integral, $E(t)$ is considered to be a piecewise continuous function over the entire integration limits and $E(t)$ changes linearly with respect to time over a given discrete time interval $[m\Delta t, (m+1)\Delta t]$ where m represents the previous m th time step of the current n th time step in the FDTD calculation [11]. Referring to Fig.1, in terms of the electric field values, E^m and E^{m+1} , which are evaluated at discrete time steps $t=m\Delta t$ and $t=(m+1)\Delta t$, respectively, we can express $E(t)$ in the following form.

$$E(t) = E^{m+1} - \frac{(E^{m+1} - E^m)}{\Delta t} (t - m\Delta t); \quad m\Delta t < t < (m+1)\Delta t < n\Delta t \quad (2.6)$$

When Eq.(2.6) is substituted into Eq.(2.4), we can obtain the following expressions for discrete values of $(P_\rho^l)^n$ at time increment n (see Appendix for manipulations).

$$(P_\rho^l)^n = \sum_{m=0}^{n-1} \{ E^{m+1} (\psi_{\rho,0}^\ell)^{n,m} - [E^{m+1} - E^m] (\psi_{\rho,1}^\ell)^{n,m} \} \quad (2.7)$$

where

$$(\psi_{\rho,0}^\ell)^{n,m} \equiv \int_{(n-1-m)\Delta t}^{(n-m)\Delta t} X_\rho^{(1)}(\tau) d\tau \quad (2.8)$$

$$(\psi_{\rho,1}^\ell)^{n,m} \equiv \frac{1}{\Delta t} \int_{(n-1-m)\Delta t}^{(n-m)\Delta t} [(n-m)\Delta t - \tau] X_\rho^{(1)}(\tau) d\tau \quad (2.9)$$

Similarly, substituting Eq.(2.6) into Eq.(2.5), we can obtain the following expressions for discrete values of $(P_\rho^{nl})^n$ at time increment n (see also Appendix for manipulations).

$$(P_\rho^{nl})^n = \sum_{m=0}^{n-1} \{ (E^{m+1})^2 (\psi_{\rho,0}^{nl})^{n,m} - 2 E^{m+1} (E^{m+1} - E^m) (\psi_{\rho,1}^{nl})^{n,m} + (E^{m+1} - E^m)^2 (\psi_{\rho,2}^{nl})^{n,m} \} \quad (2.10)$$

where

$$(\Psi_{\rho,0}^{n\ell})^{n,m} \equiv \int_{(n-1-m)\Delta t}^{(n-m)\Delta t} \chi_{\rho}^{(3)}(\tau) d\tau \quad (2.11)$$

$$(\Psi_{\rho,1}^{n\ell})^{n,m} \equiv \frac{1}{\Delta t} \int_{(n-1-m)\Delta t}^{(n-m)\Delta t} [(n-m)\Delta t - \tau] \chi_{\rho}^{(3)}(\tau) d\tau \quad (2.12)$$

$$(\Psi_{\rho,2}^{n\ell})^{n,m} \equiv \frac{1}{(\Delta t)^2} \int_{(n-1-m)\Delta t}^{(n-m)\Delta t} [(n-m)\Delta t - \tau]^2 \chi_{\rho}^{(3)}(\tau) d\tau \quad (2.13)$$

When Eq.(1.5) is substituted in Eqs.(2.8) and (2.9), and Eq.(1.6) in Eqs.(2.11), (2.12) and (2.13), we can show after some manipulations the following recursive relationships to exist between next time step $(n+1)\Delta t$ and current time step $n\Delta t$.

$$(\Psi_{\rho,0}^{\ell})^{n+1,m} = \exp(-\gamma_{\rho}^{\ell} \Delta t) (\Psi_{\rho,0}^{\ell})^{n,m} \quad (2.14)$$

$$(\Psi_{\rho,1}^{\ell})^{n+1,m} = \exp(-\gamma_{\rho}^{\ell} \Delta t) (\Psi_{\rho,1}^{\ell})^{n,m} \quad (2.15)$$

$$(\Psi_{\rho,0}^{n\ell})^{n+1,m} = \exp(-\gamma_{\rho}^{n\ell} \Delta t) (\Psi_{\rho,0}^{n\ell})^{n,m} \quad (2.16)$$

$$(\Psi_{\rho,1}^{n\ell})^{n+1,m} = \exp(-\gamma_{\rho}^{n\ell} \Delta t) (\Psi_{\rho,1}^{n\ell})^{n,m} \quad (2.17)$$

$$(\Psi_{\rho,2}^{n\ell})^{n+1,m} = \exp(-\gamma_{\rho}^{n\ell} \Delta t) (\Psi_{\rho,2}^{n\ell})^{n,m} \quad (2.18)$$

We are able to obtain the above recursive relationships only because the susceptibility functions are expressed in the exponential form.

When Eqs.(2.14) through (2.18) are used in Eqs.(2.7) and (2.10), respectively, for the next discrete time step at $(n+1)\Delta t$, we can obtain the following recursive relationships for $(P_{\rho}^{\ell})^{n+1}$ and $(P_{\rho}^{n\ell})^{n+1}$ in terms of E^{n+1} , E^n , $(P_{\rho}^{\ell})^n$ and $(P_{\rho}^{n\ell})^n$.

$$\begin{aligned} (P_{\rho}^{\ell})^{n+1} &= E^{n+1} (\Psi_{\rho,0}^{\ell})^{n+1,n} - (E^{n+1} - E^n) (\Psi_{\rho,1}^{\ell})^{n+1,n} \\ &\quad + \exp(-\gamma_{\rho}^{\ell} \Delta t) (P_{\rho}^{\ell})^n \end{aligned} \quad (2.19)$$

$$\begin{aligned} (P_{\rho}^{n\ell})^{n+1} &= (E^{n+1})^2 (\Psi_{\rho,0}^{n\ell})^{n+1,n} - 2 E^{n+1} (E^{n+1} - E^n) (\Psi_{\rho,1}^{n\ell})^{n+1,n} \\ &\quad + (E^{n+1} - E^n)^2 (\Psi_{\rho,2}^{n\ell})^{n+1,n} + \exp(-\gamma_{\rho}^{n\ell} \Delta t) (P_{\rho}^{n\ell})^n \end{aligned} \quad (2.20)$$

In the above expressions, $(\Psi_{\rho,0}^{\ell})^{n+1,n}$, $(\Psi_{\rho,1}^{\ell})^{n+1,n}$, $(\Psi_{\rho,0}^{n\ell})^{n+1,n}$, $(\Psi_{\rho,1}^{n\ell})^{n+1,n}$ and $(\Psi_{\rho,2}^{n\ell})^{n+1,n}$ are evaluated at each successive time step using the recursive relationships [see Eqs.(2.14) through (2.18)] starting with initial values of $(\Psi_{\rho,0}^{\ell})^{1,0}$, $(\Psi_{\rho,1}^{\ell})^{1,0}$, $(\Psi_{\rho,0}^{n\ell})^{1,0}$, $(\Psi_{\rho,1}^{n\ell})^{1,0}$ and $(\Psi_{\rho,2}^{n\ell})^{1,0}$, which are calculated explicitly at the beginning of computer simulation for the

selected value of Δt [see Eqs.(2.8), (2.9), (2.11), (2.12) and (2.13) and set $n=1$ and $m=0$].

To demonstrate how the above terms are used in FDTD calculations, we considered the one dimensional case where the propagating wave vector k lies along a major axis in Cartesian coordinates. The analysis can be extended easily in the three dimensional case where the EM wave is propagating in any arbitrary direction based on the following sample formulation as described below. For our one dimensional case, we arbitrarily picked the k vector to lie in the x direction, D_y and E_y field vectors in the y direction and H_z field vector in the z direction. When Eq.(2.1) is differenced in both time and space using the usual Yee algorithm, we have

$$\frac{(D_y^{n+1})_i - (D_y^n)_i}{\Delta t} = \frac{(H_z^{n+1/2})_{i+1/2} - (H_z^{n+1/2})_{i-1/2}}{\Delta x} - \frac{\sigma [(E_y^{n+1})_i + (E_y^n)_i]}{2} \quad (2.21)$$

where n and i indices are used to denote discrete n th time step $n\Delta t$ and i th spatial location $i\Delta x$, respectively.

Using Eqs.(2.3), (2.19) and (2.20), the left-hand side of Eq.(2.21) can be expressed in terms of $(E_y^{n+1})_i$ and $(E_y^n)_i$ as follow

$$\begin{aligned} (D_y^{n+1})_i - (D_y^n)_i &= \epsilon_o \epsilon_\infty [(E_y^{n+1})_i - (E_y^n)_i] \\ &+ \epsilon_o \sum_p \{ (E_y^{n+1})_i (\psi_{p,0}^\ell)^{n+1,n} - [(E_y^{n+1})_i - (E_y^n)_i] (\psi_{p,1}^\ell)^{n+1,n} \\ &\quad + [\exp(-\gamma_p^\ell \Delta t) - 1] [(P_p^\ell)^n]_i \} \\ &+ \epsilon_o \sum_p \{ [[(E_y^{n+1})_i]^3 - [(E_y^n)_i]^3] \alpha_{0p}^{(3)} + [(E_y^{n+1})_i]^3 (\psi_{p,0}^{n\ell})^{n+1,n} \\ &\quad - 2 [(E_y^{n+1})_i]^2 [(E_y^{n+1})_i - (E_y^n)_i] (\psi_{p,1}^{n\ell})^{n+1,n} \\ &\quad + (E_y^{n+1})_i [(E_y^{n+1})_i - (E_y^n)_i]^2 (\psi_{p,2}^{n\ell})^{n+1,n} \\ &\quad + [(E_y^{n+1})_i \exp(-\gamma_p^{n\ell} \Delta t) - (E_y^n)_i] [(P_p^{n\ell})^n]_i \} \end{aligned} \quad (2.22)$$

When Eq.(2.22) is substituted in Eq.(2.21), it results in the following cubic equation in which we need to solve for $(E_y^{n+1})_i$.

$$\sum_{k=0}^3 a_k [(E_y^{n+1})_i]^k = 0 \quad (2.23)$$

where

$$\begin{aligned} a_0 &\equiv -\frac{\Delta t}{\Delta x} [(H_z^{n+1/2})_{i+1/2} - (H_z^{n+1/2})_{i-1/2}] + (E_y^n)_i \frac{\sigma \Delta t}{2} - (E_y^n)_i \epsilon_o \epsilon_\infty \\ &- \epsilon_o \sum_p \{ (E_y^n)_i (\psi_{p,1}^\ell)^{n+1,n} + [1 - \exp(-\gamma_p^\ell \Delta t)] [(P_p^\ell)^n]_i \\ &\quad + [(E_y^n)_i]^3 \alpha_{0p}^{(3)} + (E_y^n)_i [(P_p^{n\ell})^n]_i \} \end{aligned} \quad (2.24)$$

$$a_1 \equiv \frac{\sigma \Delta t}{2} + \epsilon_o \epsilon_\infty + \epsilon_o \sum_{\rho} \{ (\psi_{\rho,0}^{\ell})^{n+1,n} - (\psi_{\rho,1}^{\ell})^{n+1,n} + [(E_y^n)_i]^2 (\psi_{\rho,2}^{n\ell})^{n+1,n} + \exp(-\gamma_{\rho}^{n\ell} \Delta t) [(P_{\rho}^{n\ell})^n]_i \} \quad (2.25)$$

$$a_2 \equiv \epsilon_o \sum_{\rho} \{ 2(E_y^n)_i (\psi_{\rho,1}^{n\ell})^{n+1,n} - 2(E_y^n)_i (\psi_{\rho,2}^{n\ell})^{n+1,n} \} \quad (2.26)$$

$$a_3 \equiv \epsilon_o \sum_{\rho} \{ \alpha_{0\rho}^{(3)} + (\psi_{\rho,0}^{n\ell})^{n+1,n} - 2(\psi_{\rho,1}^{n\ell})^{n+1,n} + (\psi_{\rho,2}^{n\ell})^{n+1,n} \} \quad (2.27)$$

Note that because we defined the electric susceptibility functions to be real parts of complex exponential functions as shown in Eqs.(1.5) and (1.6), it is important that we choose only the real parts when evaluating the above constants a_0 , a_1 , a_2 , and a_3 .

The above equation can be solved for $(E_y^{n+1})_i$ using any one of the root finding numerical techniques.

At each successive time step, only Eqs.(2.19), (2.20) and (2.23) have to be solved for updated $[(P_{\rho}^l)^{n+1}]_i$, $[(P_{\rho}^{n\ell})^{n+1}]_i$ and $(E^{n+1})_i$ values in order to handle the electric field response of nonlinear dispersive materials.

For the purely linear dispersive case, a_2 and a_3 , as well as some terms appearing in a_0 and a_1 , turn out to be zero. In this case we can solve for $(E_y^{n+1})_i$ directly without having to rely on the numerical root finding technique as seen in many previously published papers [12-18] that discuss computational schemes for linear dispersive materials.

III. NUMERICAL ANALYSIS - A CASE STUDY FOR NONLINEAR SOLITON FORMATION

To demonstrate the validity of the PCRC method, we investigated the case of an optical pulse where it propagated in the x-direction in free space and incident on an infinite half space dispersive medium that is characterized by zero electrical conductivity and the following single time dependent first-order (linear) and third-order (nonlinear) susceptibility functions, $X_{\rho}^{(1)}(t)$ and $\chi_{\rho}^{(3)}(t)$ [19].

For linear dispersion contribution:

$$X_{\rho}^{(1)}(t) = \frac{(\omega_R)^2}{v_o} \exp(-\delta t) \sin(v_o t) \quad (3.1)$$

For nonlinear dispersion contribution arising from purely Raman scattering and no virtual electronics transition effect [20]:

$$\chi_{\rho}^{(3)}(t) = \chi_o^{(3)} [(\tau_1^2 + \tau_2^2)/\tau_1 \tau_2] \exp(-t/\tau_2) \sin(t/\tau_1) \quad \text{and} \quad \alpha_{0\rho}^{(3)} = 0 \quad (3.2)$$

where $\omega_R^2 \equiv \omega_o^2(\epsilon_s - \epsilon_\infty)$, $v_o \equiv \sqrt{(\omega_o^2 - \delta^2)}$, ω_o is the resonant frequency, ϵ_s is relative permittivity at DC, δ is the first-order susceptibility damping constant, $\chi_o^{(3)}$ is the nonlinear coefficient, $1/\tau_1$ is the optical phonon frequency, and τ_2 is the optical phonon

lifetime.

Comparing Eqs.(3.1) and (3.2) with the previously defined susceptibility functions as seen in Eqs.(1.5) and (1.6), we can relate the above coefficients to the previously defined susceptibility coefficients as follows.

$$\alpha_p^\ell \Leftarrow i\omega_R^2/\nu_o \quad \text{and} \quad \gamma_p^\ell \Leftarrow (\delta + i\nu_o), \quad (3.3)$$

$$\alpha_p^{nl} \Leftarrow i\chi_o^{(3)} [(\tau_1^2 + \tau_2^2)/\tau_1\tau_2^2] \quad \text{and} \quad \gamma_p^{nl} \Leftarrow \left(\frac{1}{\tau_2} + i\frac{1}{\tau_1}\right). \quad (3.4)$$

where i is the imaginary number defined as $\sqrt{-1}$.

The incident optical pulse is assumed to propagate at the sinusoidal-carrier electric field frequency, ω_c , of 8.61×10^{14} rad/sec with the unit amplitude (1.0 volts/meter), enveloped inside the hyperbolic secant function represented by characteristic time constant T_w . T_w is the parameter used to determine the width of the overall shape of the incident optical pulse. Thus, we used the following expression to launch the incident optical pulse in free space for our FDTD simulation.

$$\text{Incident Optical Pulse } (t) = \cos [\omega_c (t - t_{delay})] \operatorname{sech} \left[\frac{(t - t_{delay})}{T_w} \right] \quad (3.5)$$

where t_{delay} is the delay time for the incident optical pulse to reach the peak value at the place where the optical pulse is launched. Two different values of the characteristic time constant are used to investigate the effect of the characteristic time constant on soliton formation. We used 3.5 femtoseconds (fs) and 7.0 fs for the characteristic time constants. These characteristic time constants resulted in enveloping about 6 cycles of the electric field oscillation for the 3.5 fs pulse and 12 cycles for the 7.0 fs pulse.

We selected the total simulation cells to be 50,000, ranging from $x=-10,000$ to $x=40,000$ with the free space-dispersive material interface located at $x=0$. The optical pulse was launched in free space at $x=-10,000$, traveling in the positive x direction. The LIAO absorbing boundary condition [21] was used at the two end points of the computational space.

For the selection of basic FDTD parameters we chose the following values.

Uniform cell size (or Δx) = 5.0 nanometers ($= 2\pi c/\omega_c/438 = \lambda_c/438$),

Time step increment (or Δt) = 8.33 attoseconds (10^{-18}) ($= \Delta x/2c$),

Total number of uniform cells = 50,000,

Total number of time steps = 2×10^5 ,

where c is the speed of light. For Δx of 5 nanometers, we can estimate the free space numerical phase velocity error to be around 5×10^{-6} [22].

To observe the soliton formation within the total propagation distance of 250 micrometers ($= 5.0$ nanometers/cell \times 50,000 cells), we had to enhance the nonlinear behavior by scaling the coefficients found in the first and third order susceptibility functions (see Eqs.(3.1) and (3.2)). To show consistencies of our FDTD results with previously published results, we used the values similar to the ones found in the papers

referenced in [4,5]. Shown below are the values that we used for our FDTD calculations.

For linear dispersive material properties:

$$\begin{aligned}\epsilon_s &= 5.25; \epsilon_\infty = 2.25; \\ \omega_o &= 8 \times 10^{14} \text{ sec}^{-1}; \delta = 4.0 \times 10^9 \text{ sec}^{-1}.\end{aligned}$$

For nonlinear dispersive material properties:

$$\begin{aligned}\chi_o^{(3)} &= 30.0 \text{ (volts/meter)}^2; \\ \tau_1 &= 12.2 \text{ fs}; \tau_2 = 32.0 \text{ fs}.\end{aligned}$$

To see the difference in linear and nonlinear responses, we first calculated the linear dispersive case by setting the nonlinear coefficient, $\chi_o^{(3)}$, to zero. For the nonlinear case, we used the nonlinear material property values as shown above.

To calculate the updated electric field value at each time step, we used the simple Newton iteration method by making use of the previous time step electric field value as the initial guess to solve the cubic equation (see Eq.(2.23)). For every simulation we performed, the convergence criterion of 10^{-4} was reached after at most two iterations.

Shown in Fig.2 and Fig.3 are spatial plots obtained for linear and nonlinear dispersive calculations, respectively, at time steps of 10,000, 40,000, 70,000, 100,000 and 130,000 for the incident optical pulse width of 3.5 fs. Similarly, Fig.4 and Fig.5 show spatial plots obtained for the same input values with the exception of 7.0 fs, instead of 3.5 fs, for the incident optical pulse width. As seen in Fig.2 and Fig.3 (likewise Fig.4 and Fig.5) the solitary wave started forming first with the appearance of the small spike-like shape inside the linearly dispersive part of the pulse as a result of the nonlinear self-focusing effect. As the pulse propagated deeper in the dispersive medium, the spike-like shape transformed gradually to the shape that resembles the solitary wave packet and became isolated from the main linear dispersive part of the pulse due to the slower phase velocity. Once the solitary wave packet became completely isolated from the linear dispersive part of the pulse, the solitary wave packet propagated at constant amplitude while maintaining the general structure. On the other hand, the linear dispersive part of the pulse decreased in its amplitude and became much broader in its shape as it propagated deeper into the dispersive medium because of the linear dispersive effect.

Shown Fig.6 is the comparison of two solitary wave packets that are formed from the two different incident optical pulse widths. It shows the overlay views taken around solitary wave packets of the two spatial plots which are found in Fig.3 and Fig.5 (specifically at the time step of 100,000). We can see that these two solitary wave packets have approximately the same size envelopes. We estimated the solitary wave packet sizes to be around 1.54 micrometers based on approximately two wave cycles of oscillation at a wavelength of 0.77 micrometers contained inside the envelopes of these solitary wave packets. We can think of that the formation of the same size solitary wave packet is analogous to calculating the allowable bound states of the nonlinear Schrodinger wave equation inside a potential well [23]. Because of material property values used for our simulation calculations, we ended up getting the unique solitary wave packet size as we saw in our simulation results.

Also shown in Fig.6 is the difference we obtained in the amplitude of the two solitary wave packets from two different incident optical pulse widths. The wider incident pulse resulted in about 1.2 times that of the narrow incident pulse.

For the nonlinear case, we saw the formation of a small secondary high frequency pulse that moved ahead of both the linear dispersive part of the pulse and the nonlinear solitary wave packet. The same secondary high frequency pulse was also obtained and reported previously for computational modeling of femtosecond optical solitons using another FDTD approach, called the auxiliary differential equation approach, to handle the nonlinear dispersive term.

To perform these calculations we used a SPARC 20 workstation equipped with a 75 MHz processor and 512 Megabyte dynamic random access memory chips. On average it took around 24 CPU hours to complete the job with no optimization. There was little difference in the total computational time for the linear dispersive case as compared to the nonlinear dispersive case. Using present day computers equipped with much faster multiple processors, the computational time can be reduced considerably more.

IV. CONCLUSIONS

In conclusion, we have shown in our sample calculations that the PCRC approach of the FDTD method presented here is fully capable of predicting the formation of nonlinear solitary waves by solving Maxwell's equations directly. The PCRC approach resulted in a much simpler algebraic form to relate the displacement field vector to the electric field vector than the auxiliary differential equation approach which requires the additional coupled nonlinear ordinary equations to be solved at each time step. Consequently, the PCRC approach is capable of calculating at much faster computational speed. Also, because of the piecewise linear approximation used for the time dependent electric field vector, the PCRC approach should provide the accuracy comparable to that of the auxiliary differential equation approach.

Also, we gained much from exponential function forms of the linear and nonlinear susceptibility functions which allowed us to implement the recursive feature in our algorithm. As a whole, the PCRC approach retained all the advantages of the usual discrete recursive convolution approach, such as fast computational speed and efficient use of the computer memory, however, with much improved accuracy.

The nonlinear dispersive formulation resulted in having to solve the cubic equation for the successive time step electric field values as compared to the linear equation for the simple linear dispersive case. For sample calculations we have looked into here, the simple Newton iterative method provided sufficiently fast convergence for finding the root of the cubic equation by using the previous time step electric field value as the initial guess.

The present PCRC approach is robust and applicable for applications in two and three dimensional problems. The one dimensional code can be extended easily into two and three dimensional codes with little effort.

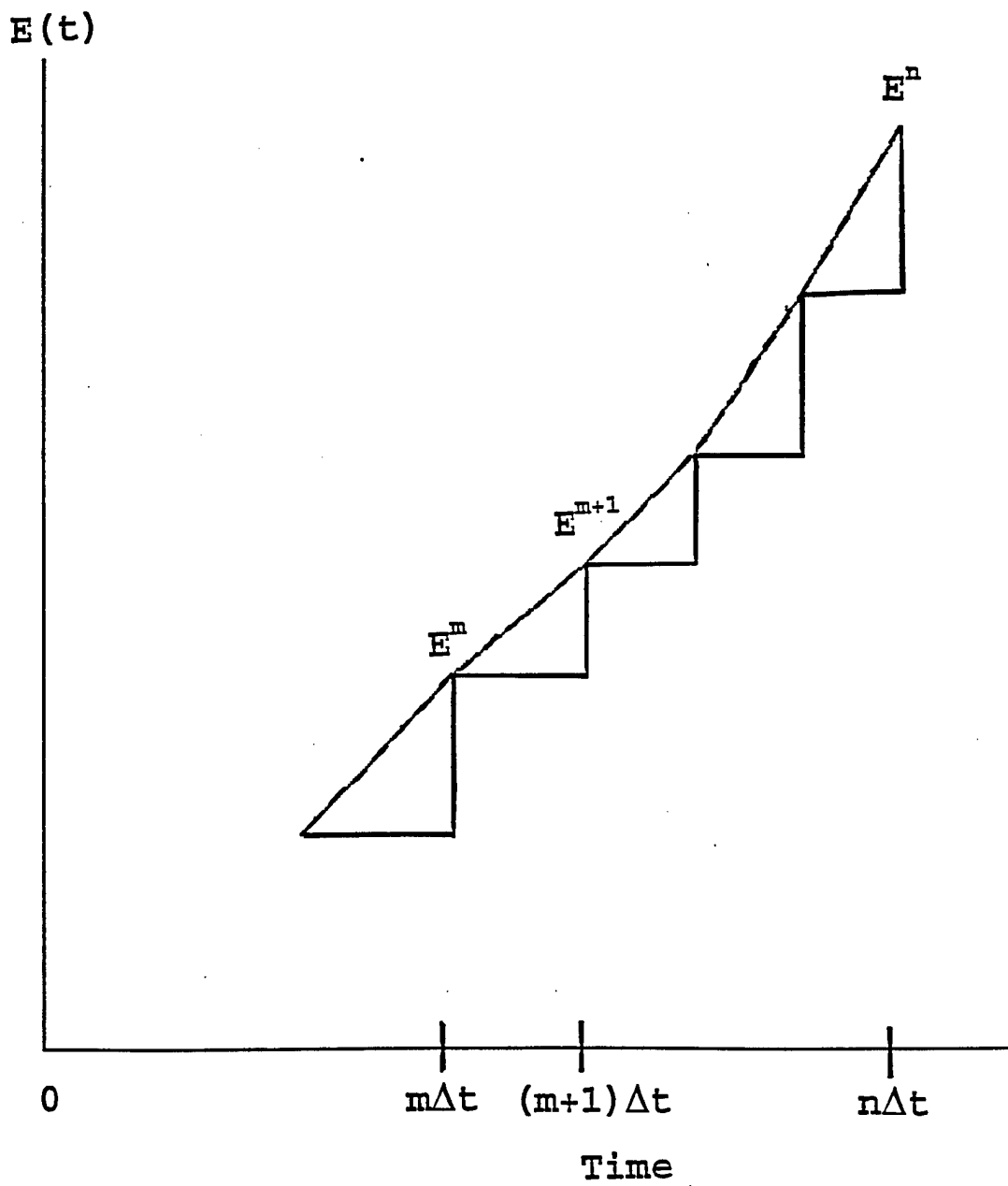


Fig. 1. Illustration of Piecewise Linear Approximation for the Electric Field as a Function of Discrete Time Steps

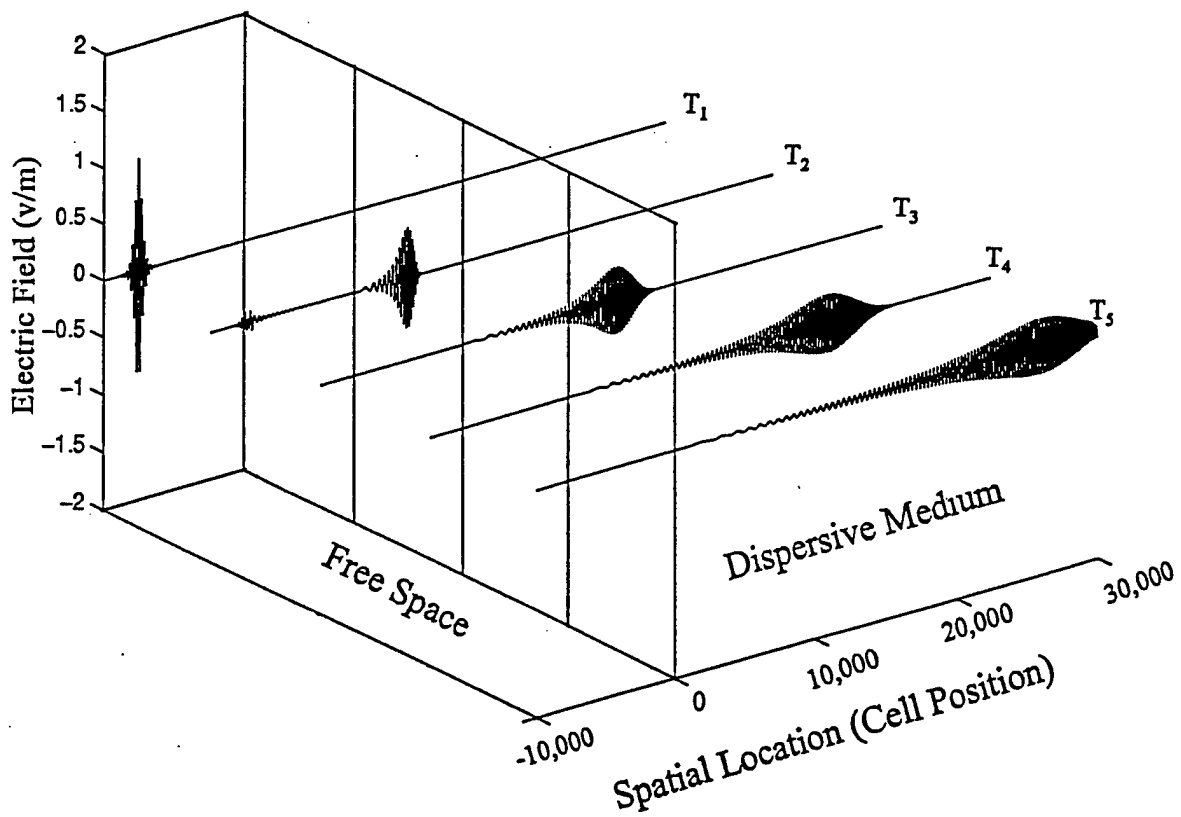


Fig. 2. Perspective plots of the electric field intensity versus spatial location from linear dispersive calculations taken at five successive times of T_1, T_2, T_3, T_4 and T_5 in order to show the space-time evolution of the optical pulse with the initial pulse width of 3.5 fs.

[$T_1 = 10,000\Delta t (=0.083 \text{ ps})$; $T_2 = 40,000\Delta t (=0.333 \text{ ps})$;
 $T_3 = 70,000\Delta t (=0.583 \text{ ps})$; $T_4 = 100,000\Delta t (=0.833 \text{ ps})$;
 $T_5 = 130,000\Delta t (=1.083 \text{ ps})$ with $\Delta t = 8.33 \times 10^{-18}$ second]

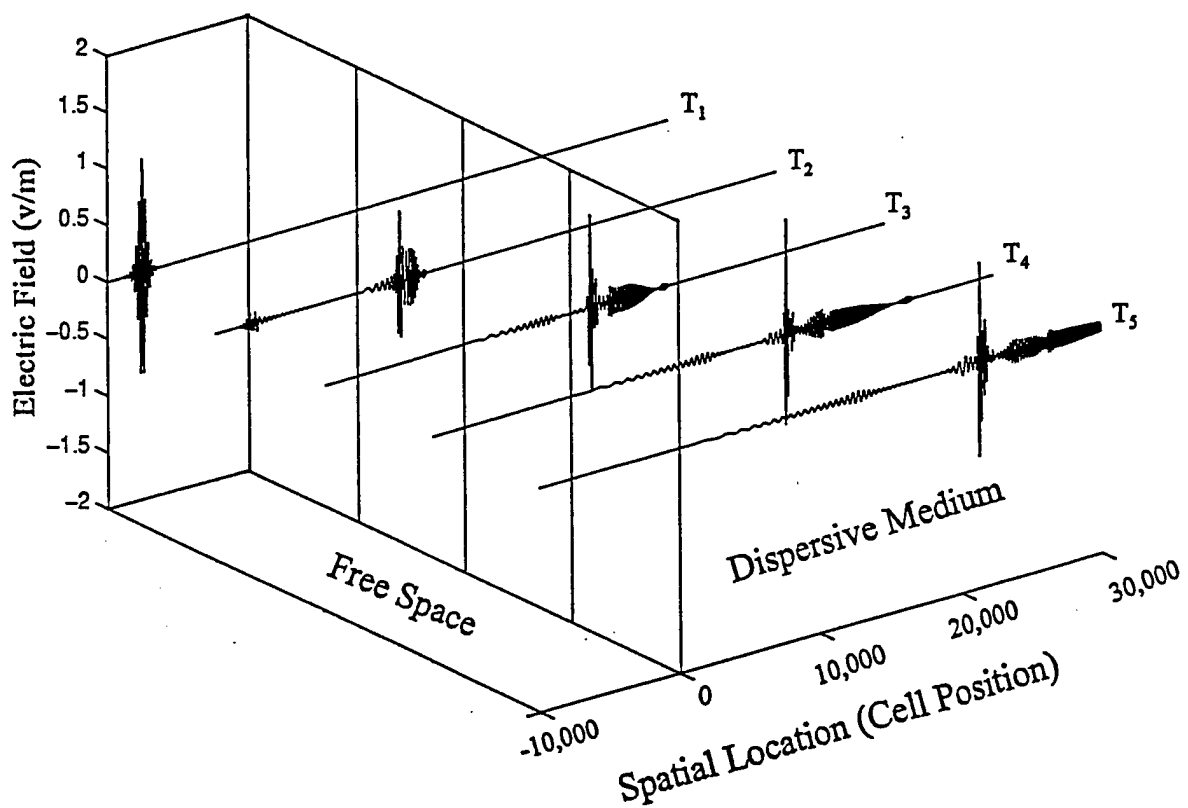


Fig. 3. Perspective plots of the electric field intensity versus spatial location from nonlinear dispersive calculations taken at five successive times of T_1 , T_2 , T_3 , T_4 and T_5 in order to show the space-time evolution of the optical pulse with the initial pulse width of 3.5 fs.

[$T_1 = 10,000\Delta t$ ($=0.083$ ps); $T_2 = 40,000\Delta t$ ($=0.333$ ps);
 $T_3 = 70,000\Delta t$ ($=0.583$ ps); $T_4 = 100,000\Delta t$ ($=0.833$ ps);
 $T_5 = 130,000\Delta t$ ($=1.083$ ps) with $\Delta t = 8.33 \times 10^{-18}$ second]

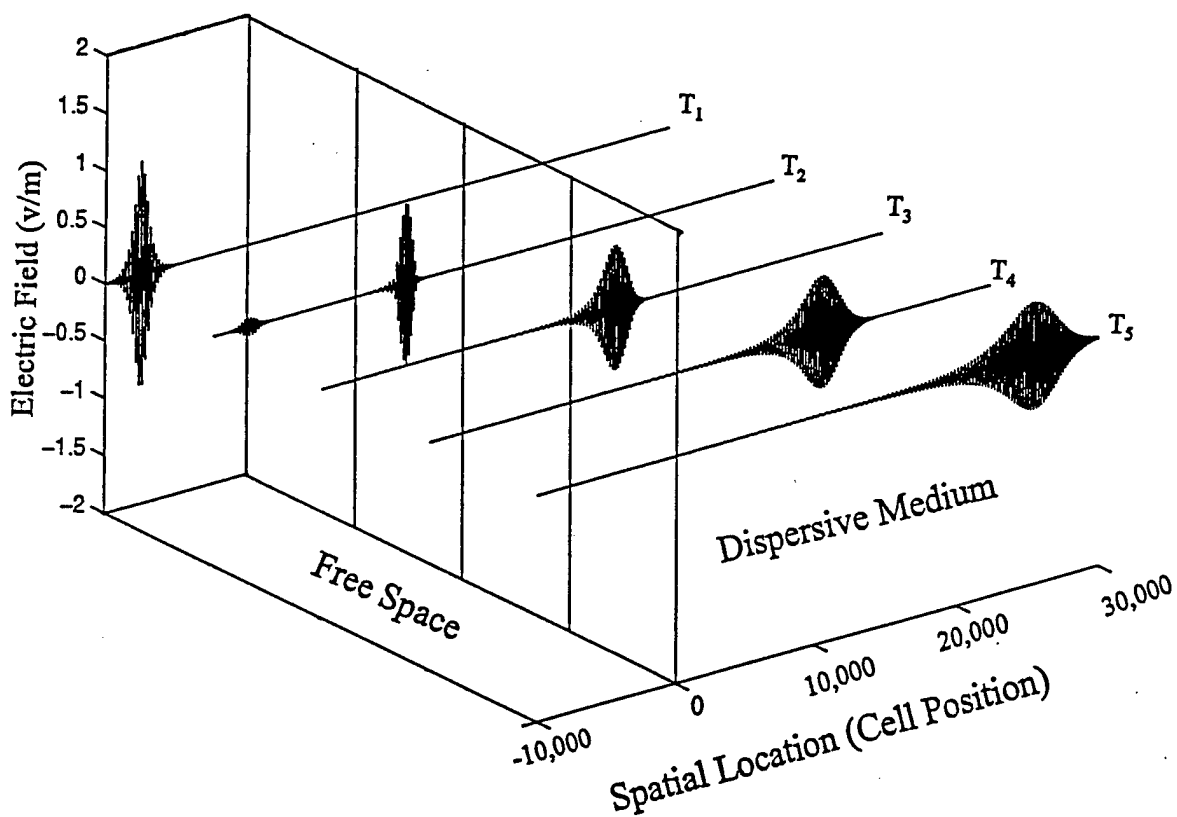


Fig. 4. Perspective plots of the electric field intensity versus spatial location from linear dispersive calculations taken at five successive times of T_1 , T_2 , T_3 , T_4 and T_5 in order to show the space-time evolution of the optical pulse with the initial pulse width of 7.0 fs.

[$T_1 = 10,000\Delta t$ ($=0.083$ ps); $T_2 = 40,000\Delta t$ ($=0.333$ ps);
 $T_3 = 70,000\Delta t$ ($=0.583$ ps); $T_4 = 100,000\Delta t$ ($=0.833$ ps);
 $T_5 = 130,000\Delta t$ ($=1.083$ ps) with $\Delta t = 8.33 \times 10^{-18}$ second]

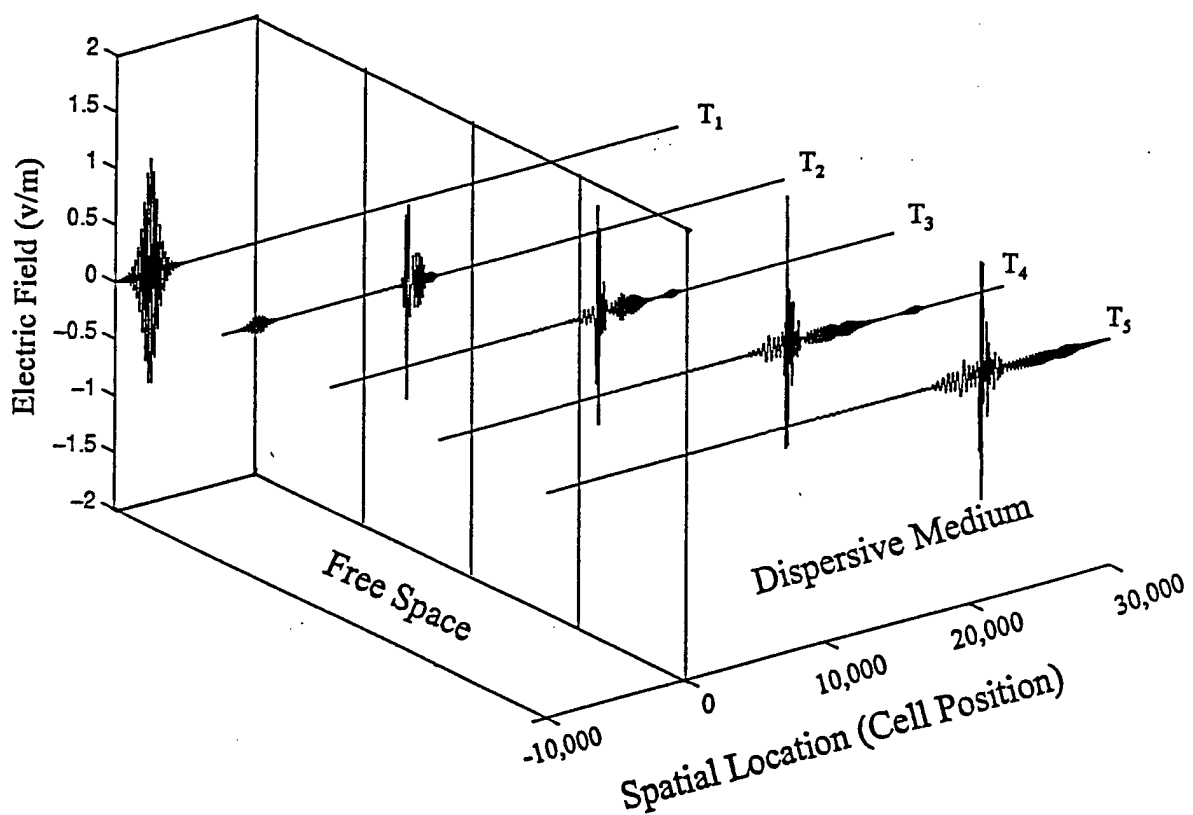


Fig. 5. Perspective plots of the electric field intensity versus spatial location from nonlinear dispersive calculations taken at five successive times of T_1 , T_2 , T_3 , T_4 and T_5 in order to show the space-time evolution of the optical pulse with the initial width of 7.0 fs.

[$T_1 = 10,000\Delta t$ ($=0.083$ ps); $T_2 = 40,000\Delta t$ ($=0.333$ ps);
 $T_3 = 70,000\Delta t$ ($=0.583$ ps); $T_4 = 100,000\Delta t$ ($=0.833$ ps);
 $T_5 = 130,000\Delta t$ ($=1.083$ ps) with $\Delta t = 8.33 \times 10^{-18}$ second]

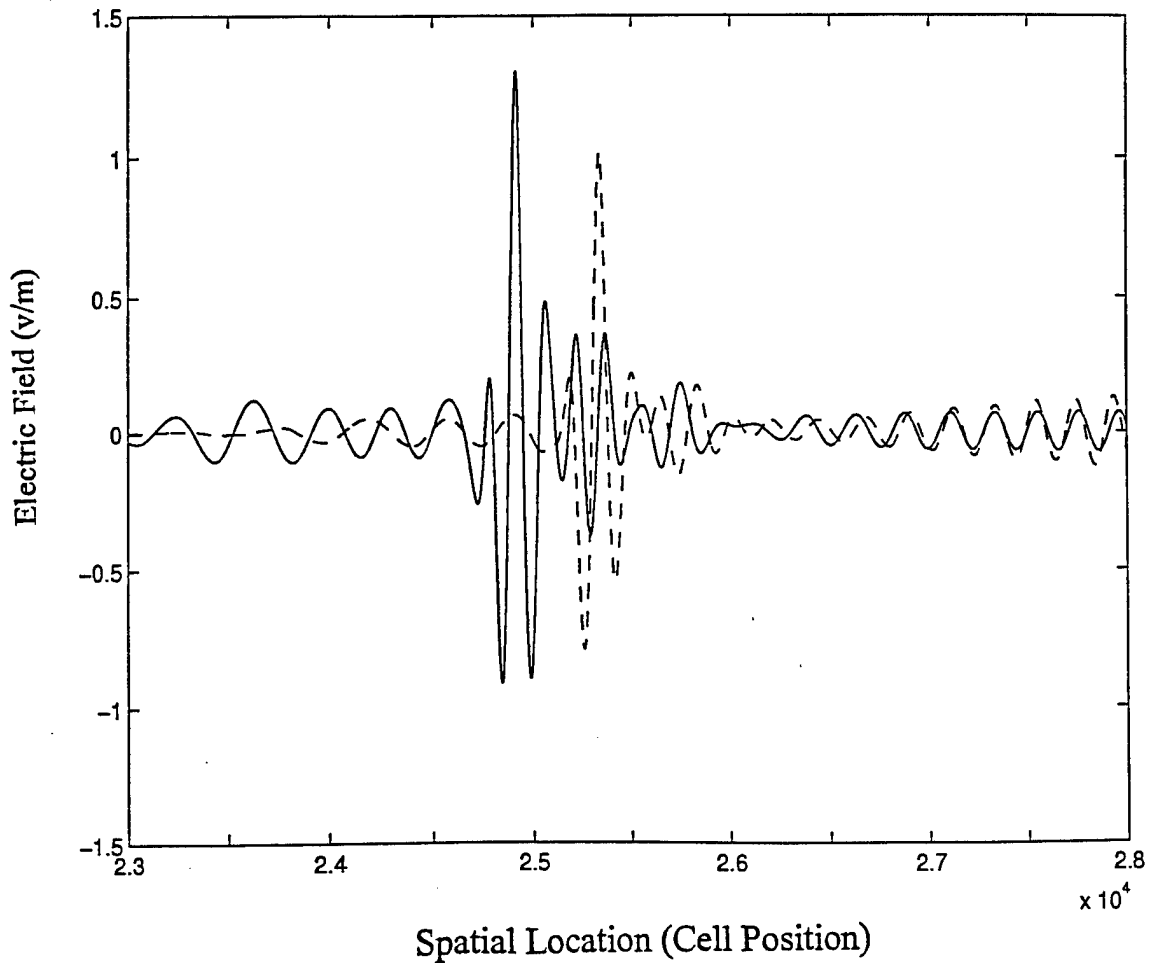


Fig. 6. Comparison of solitary wave packets obtained in the nonlinear dispersive medium from launching two different width pulses in free space. The solid line is from the optical pulse width of 7.0 fs and the dashed line is from the optical pulse width of 3.5 fs. These are taken at the time step of 100,000.

REFERENCES

- [1] T-H. Huang, C-C. Hsu, T-H. Wei, S. Chang, S-M Yen, C-P. Tsai, R-T. Liu, C-T. Kuo, W-S. Tse and C. Chia, "The Transient Optical Kerr Effect of Simple Liquids Studied with an Ultrashort Laser with Variable Pulsewidth," *IEEE Jour. of Selected Topics in Quantum Electronics*, vol 2, pp. 756-775, 1996
- [2] K. J. Blow and D. Wood, "Theoretical Description of Transient Stimulated Raman Scattering in Optical Fibers," *IEEE Jour. of Quantum Electronics*, vol 25, pp. 2665-2673, 1989
- [3] K. S. Yee, "Numerical Solution of Initial Boundary Value Problems Involving Maxwell's Equations in Isotropic Media," *IEEE Trans. Antenna Propagat.*, vol AP-14, pp. 302-307, 1966.
- [4] P. M. Goorjian, A. Taflove, R. M. Joseph and S.C. Hagness, "Computational Modeling of Femtosecond Optical Solitons from Maxwell's Equations," *IEEE J. of Quantum Electronics*, vol 28, pp. 2416-2422, 1992
- [5] P. M. Goorjian, A. Taflove, "Direct Time Integration of Maxwell's Equations in Nonlinear Dispersive Media for Propagation of Femtosecond Electromagnetic Solitons," *Opt. Lett.*, vol 17, pp. 180-182, 1992
- [6] R. M. Joseph, P. M. Goorjian and A. Taflove, "Direct Time Integration of Maxwell's Equations in Two-Dimensional Dielectric Waveguides for Propagation and Scattering of Femtosecond Electromagnetic Solitons," *Opt. Lett.*, vol 18, pp. 491-493, 1993
- [7] R. M. Joseph and A. Taflove, "Spatial Soliton Deflection Mechanism Indicated by FD-TD Maxwell's Equations Modeling," *IEEE Photonics Tech. Lett.*, vol 6, pp. 1251-1254, 1994
- [8] R. W. Ziolkowski and J. B. Judkins, "Applications of the Nonlinear Finite Difference Time Domain (NL-FDTD) Method to Pulse Propagation in Nonlinear Media: Self Focusing and Linear Interfaces," *Opt. Lett.*, vol 18, pp. 491-493, 1993
- [9] R. W. Ziolkowski and J. B. Judkins, "Full-wave Vector Maxwell Modeling of the Self-focusing of Ultrashort Optical Pulses in a Nonlinear Kerr Medium Exhibiting a Finite Response Time," *Jour. Opt. Soc. Am B.*, vol 10, pp. 186-198, 1993
- [10] R. W. Hellworth, "Third-order Optical Susceptibility of Liquids and Solids," *Prog. Quantum Electronics*, vol 5, pp. 1-68, 1977

- [11] D. F. Kelley and R. J. Luebbers, "Piecewise Linear Recursive Convolution for Dispersive Media Using FDTD," *IEEE Trans. Antenna and Propagat.*, vol 44, pp. 792-797, 1996
- [12] R. J. Luebbers, F. Hunsberger and K. S. Kunz, "A Frequency-dependent Finite Difference Time-Domain Formulation for Transient Propagation in Plasma," *IEEE Trans. Antennas and Propagat.*, vol 39, pp. 29-34, 1991
- [13] R. M. Joseph, S. C. Hagness and A. Taflove, "Direct Time Integration of Maxwell's Equations in Linear Dispersive Media with Absorption for Scattering and Propagation of Femtosecond Electromagnetic Pulses," *Opt. Lett.*, vol 16, 1412-1414, 1991
- [14] R. J. Luebbers and F. Hunsberger, "FDTD for Nth-order Dispersive Media," *IEEE Trans. Antenna and Propagat.*, vol 40, pp. 1297-1301, 1992
- [15] F. Hunsberger, R. Luebbers and K. Kunz, "Finite-Difference Time-Domain Analysis of Gyrotropic Media-I: Magnetic Plasma," *IEEE Trans. Antennas and Propagat.*, vol 40, pp. 1489-1495, 1992
- [16] R. Luebbers, D. Steich and K. Kunz, "FDTD Calculation of Scattering from Frequency-dependent Materials," *IEEE Trans. Antennas and Propagat.*, pp. 1249-1257, 1993
- [17] J. L. Young, "Propagation in Linear Dispersive Media: Finite Difference Time-Domain Methodologies," *IEEE Trans. Antennas and Propagat.*, vol 43, pp. 411-430, 1995
- [18] C. L. Holloway, "Finite-Difference Time-Domain Modeling for Field Predictions Inside Rooms," 1977 IEEE International Symposium on Electromagnetic Compatibility, August 18-22, 1997, Austin, TX
- [19] Allen Taflove, *Computational Electromagnetics: The Finite-Difference Time-Domain Method*, Boston: Artech House, 1995, pp. 230
- [20] S. A. Akmanhov, K. N. Dravovich, A. P. Sukhorukov and A. S. Chirkin, "Stimulated Raman Scattering in a Field of Ultrashort Light Pulses," *Sov. Phys.-JETP*, vol 32, pp. 266-273, 1971
- [21] Z. P. Liao, H. L. Wong, B. P. Yang and Y. F. Yuan, "A Transmitting Boundary for Transient Wave Analysis," *Scientia Sinica*, vol XXVII, pp. 1063-1076, 1984
- [22] Allen Taflove, *Computational Electromagnetics: The Finite-Difference Time-Domain Method*, Boston: Artech House, 1995, pp. 42-44

- [23] K. E. Lonngren, "Observations of Solitons on Nonlinear Dispersive Transmission Lines," *Solitons in Action*, pp. 127-152, Edited by K. Lonngren and A. Scott, Academic Press, 1978

APPENDIX

For the linear part, when we substitute Eq.(2.6) in Eq.(2.4) and evaluate t at $n\Delta t$ for the argument of the susceptibility function where n is the n th time step, we have

$$\begin{aligned}
 (P_\rho^\ell)^n &= \sum_{m=0}^{n-1} \int_{m\Delta t}^{(m+1)\Delta t} \left\{ E^{m+1} - (E^{m+1} - E^m) \frac{1}{\Delta t} [\tau - m\Delta t] \right\} X_\rho^{(1)}(n\Delta t - \tau) d\tau \\
 &= \sum_{m=0}^{n-1} \left\{ E^{m+1} \int_{m\Delta t}^{(m+1)\Delta t} X_\rho^{(1)}(n\Delta t - \tau) d\tau \right. \\
 &\quad \left. - (E^{m+1} - E^m) \frac{1}{\Delta t} \int_{m\Delta t}^{(m+1)\Delta t} [\tau - m\Delta t] X_\rho^{(1)}(n\Delta t - \tau) d\tau \right\} \quad (A.1)
 \end{aligned}$$

Similarly for the nonlinear part, when we substitute Eq.(2.6) in Eq.(2.5) and evaluate t at $n\Delta t$ for the argument of the susceptibility function where n is the n th time step, we have

$$\begin{aligned}
 (P_\rho^{n\ell})^n &= \sum_{m=0}^{n-1} \int_{m\Delta t}^{(m+1)\Delta t} \left\{ (E^{m+1})^2 - 2 E^{m+1} (E^{m+1} - E^m) \frac{1}{\Delta t} \right. \\
 &\quad \left. + (E^{m+1} - E^m)^2 \frac{1}{(\Delta t)^2} [\tau - m\Delta t]^2 \right\} \chi_\rho^{(3)}(n\Delta t - \tau) d\tau \\
 &= \sum_{m=0}^{n-1} \left\{ (E^{m+1})^2 \int_{m\Delta t}^{(m+1)\Delta t} \chi_\rho^{(3)}(n\Delta t - \tau) d\tau \right. \\
 &\quad - 2 E^{m+1} (E^{m+1} - E^m) \frac{1}{\Delta t} \int_{m\Delta t}^{(m+1)\Delta t} [\tau - m\Delta t] \chi_\rho^{(3)}(n\Delta t - \tau) d\tau \\
 &\quad \left. + (E^{m+1} - E^m)^2 \frac{1}{(\Delta t)^2} \int_{m\Delta t}^{(m+1)\Delta t} [\tau - m\Delta t]^2 \chi_\rho^{(3)}(n\Delta t - \tau) d\tau \right\} \quad (A.2)
 \end{aligned}$$

Using the change of variable $\tau' = (n\Delta t - \tau)$, we can readily show the existence of the following relationships for the above integrals

$$\int_{m\Delta t}^{(m+1)\Delta t} [\tau - m\Delta t]^k f(n\Delta t - \tau) d\tau = \int_{(n-1-m)\Delta t}^{(n-m)\Delta t} [(n-m)\Delta t - \tau']^k f(\tau') d\tau' \quad (A.3)$$

where k takes the values of 0, 1, and 2 and $f(t)$ represents, respectively, the time-dependent first and third order susceptibility functions, $X_\rho^{(1)}(t)$ and $\chi_\rho^{(3)}(t)$.

Since τ' appearing in the right-hand side of Eq.(A.3) is the integration variable, we can simply replace it by τ . When Eq.(A.3) is substituted back in Eqs.(A.1) and (A.2), we can obtain the expressions as shown in Eqs.(2.7) and (2.10).

DISTRIBUTION LIST

AUL/LSE
Bldg 1405 - 600 Chennault Circle
Maxwell AFB, AL 36112-6424 1 cy

DTIC/OCF
8725 John J. Kingman Rd, Suite 0944
Ft Belvoir, VA 22060-6218 2 cys

AFSAA/SAI
1580 Air Force Pentagon
Washington, DC 20330-1580 1 cy

AFRL/PSOT/TL
Kirtland AFB, NM 87117-5776 2 cys

AFRL/PSOT/HO
Kirtland AFB, NM 87117-5776 1 cy

AFRL/DEHE/Dan McGrath
Kirtland AFB, NM 87117-5776 1 cy

AFRL/DEPE
Kirtland AFB, NM 87117-5776 1 cy

AFRL/DEPE/Jeff McGillivray
Kirtland AFB, NM 87117-5776 5 cys

Official Record Copy
AFRL/DEPE/S. Joe Yakura
Kirtland AFB, NM 87117-5776 5 cys

